Calculation of a Vessel Scattering Acoustic Field By Using Prolate Spheroid Model

Jingxin Ma， Jianjun Zhu, Haisen Li*, Xiaodong Wang
1. Acoustic Science and Technology Laboratory, Harbin Engineering University
2. College of Underwater Acoustic Engineering, Harbin Engineering University
Harbin, China
*Corresponding author email: hsli@hrbeu.edu.cn

***Abstract*—When the vector sensors are installed in the vessels for profiling, the vectors are subject to the signals' acoustic scattering of the boundary, the vessel and water surface scattering acoustic waves maybe influence the accuracy of acoustically parameter estimation. In this paper, the prolate spheroid baffle is selected as a vessel model, the scattering of plane acoustic wave from a prolate spheroid baffle which located at the water-air surface is considered. The expressions of sound pressure field and vibration velocity field near the baffle, using the method of complex images, are derived. The scattering acoustic field of prolate spheroid baffle at different frequencies and directions in incident wave are analyzed, and the acoustic energy flow of baffle acoustic scattering field at a single point with different incident angle is calculated.**

Keyword*—*prolate spheroid baffle; acoustic scatter; image method;

I. INTRODUCTION

The baffle acoustic scattering problems that results from an incident plane wave or point source has been previously considered. The method of T-matrix, the incident and scattered wave fields are expanded in terms of a basis set with regular and outgoing functions[1-5].The method of combining with finite element method (FEM) and boundary element method (BEM) can calculate acoustic diffraction of any complex shape[6]. V.K Varadam and L. Flax etal using T-matrix calculated the rigid body scattering by prolate spheroid[4,5]. John Bartan developed a general spheroidal coordinate separation-of-variables solution for the determination of the near-field acoustic pressure distribution of a rigid spheroid at arbitrary monofrequency incident wave [7]. Ji Jianfei using finite element method developed prolate spheroid baffle model, calculated the directivity of pressure and vibration velocity of scattering acoustic field at different frequencies [8,9]. Sheng Xueli considered a closed spherical air cavity and studied its influences of the baffle acoustic scattering[10]. John A. Fawcett considered that a spherical baffle near the boundary, in the half-space using the method of complex images computed the conversion coefficients of outgoing spherical harmonic into incident spherical harmonic after a seabed reflection[11-13].

In acoustic scattering problems，the scattering body usually in free field or in the half-space near the boundary[14-16]. The study presented in this paper, the prolate spheroid at both ends of interface is considered. In the soft boundary conditions, the pressure and vibration velocity of acoustic scattering of prolate spheroid body in different direction and frequencies incident monofrequency wave is calculated.

II. PRINCIPLE

A model schematic of the prolate spheroid geometrical arrangement is given in Fig. 1. In prolate spheroidal coordinates, a is the length of the major axis and b is the length of the minor axis is b, so the focal length of the spheroid $c=(a^2-b^2)^{1/2}$, the water-air interface at the y=0,(y>0 is air, y<0 is water). For plane wave incidence, the plane wave is assumed to propagate with point (r,θ_0,φ_0) in spherical coordinates, as shown in Fig. 1. The vector sensor location is (ξ,η,φ)

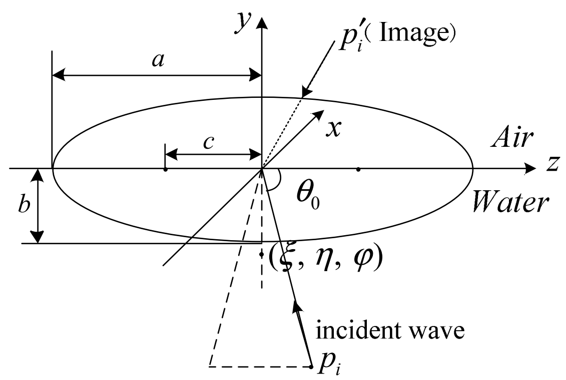

Fig. 1 The spheroid is axisymmetric about the z axis. For the prolate spheroid (as shown) the major axis is along the z axis. (y>0 is air, y<0 is water). The orientation coordinates of

incident wave in spherical coordinates is (r,θ_0,φ_0) .

Since the vessel baffle interface and water surface can be considered as rigid and soft boundary, and the acoustic field consists of a sum of the incident and scattered fields. The boundary conditions contain water surface($\eta=0,\xi>\xi_0$) and baffle interface($\xi=\xi_0$) of the time-independent Helmholtz equation:

$$\nabla^2 p+h^2 p=0 \tag{1}$$

are

$$p\big|_{\eta=0,\xi>\xi_0}=0\ ,\ \left.\frac{\partial p}{\partial\xi}\right|_{\xi=\xi_0}=0 \tag{2}$$

The corresponding expression of the observation position (ξ,η,φ) for the incident acoustic pressure is thus:

$$p_i(\vec{\mathrm{r}})=\exp\left(-jkr\left(\cos\theta\cos\theta_0+\sin\theta\sin\theta_0\cos(\varphi-\varphi_0)\right)\right) \tag{3}$$

And the incident plane pressure wave computation by the spheroidal wave functions:

$$p_i=2\sum_{n=0}^{\infty}\sum_{m=0}^{\infty}i^n\frac{2-\delta_{0m}}{N_{mn}}R_{mn}^{(1)}(h,\xi)S_{mn}(h,\eta_0)S_{mn}(h,\eta)\cdot\cos m(\varphi-\varphi_0+\pi) \tag{4}$$

where $R_{mn}^{(1)}(h,\varepsilon)$ and $S_{mn}(h,\eta)$ are the radial and the angular spheroidal wave functions of the first kind. $\eta_0=\cos\theta_0$, where θ_0 and φ_0 are the orientation coordinates of incident wave in spherical coordinates. $h=kc=2\pi c/\lambda$ is the spheroidal size parameter, where k is the wave number.. Where N_{mn} is a constant that can be determined from the associated spheroidal function parameters[17].

$$N_{mn}=\int_{-1}^{1}[S_{mn}(h,\eta)]^2 d\eta=2\sum_{r=0'1'}^{\infty}\frac{(r+2m)!(d_r^{mn})^2}{(2r+2m+1)r!} \tag{5}$$

Where the summation is over even integers if (*n-m*) is even and is over odd integers if (*n-m*) is odd.

The questions of the prolate spheroid's scattered fields at the water-air interface can be considered as the prolate spheroid in water free field with two sound sources. The water-air interface's scattering can be considered as an image source p_i' , incident acoustic source and image source, as shown in Fig. 1, will satisfied the water-air interface soft boundary condition.

$$p_i'(\vec{\mathrm{r}})=\exp\left(-jkr\left(\cos\theta\cos\theta_0+\sin\theta\sin\theta_0\cos(\varphi+\varphi_0)\right)\right) \tag{6}$$

And the image incident plane pressure wave computation by the spheroidal wave functions:

$$p_i'=-2\sum_{n=0}^{\infty}\sum_{m=0}^{\infty}i^n\frac{2-\delta_{0m}}{N_{mn}}R_{mn}^{(1)}(h,\xi)S_{mn}(h,\eta_0)S_{mn}(h,\eta)\cdot\cos m(\varphi+\varphi_0-\pi) \tag{7}$$

Thus, the prolate spheroid's near fields under the water interface will be $p=p_i+p_i'+p_s$, at prolate spheroid baffle interface($\xi=\xi_0$),

$$\left.\frac{\partial\left(p_i+p_i'+p_s\right)}{\partial\xi}\right|_{\xi=\xi_0}=0 \tag{8}$$

The Eq(4) and Eq(7) are substituted into the boundary condition Eq(8), the series terms of p_s will be:

$$p_s=-4\sum_{n=0}^{\infty}\sum_{m=0}^{\infty}i^n\frac{(2-\delta_{0m})R_{mn}^{(1)\prime}(c,\xi_1)}{N_{mn}R_{mn}^{(3)\prime}(c,\xi_1)}R_{mn}^{(3)}(h,\xi)S_{mn}(h,\eta_0)\cdot S_{mn}(h,\eta)\sin(\mathrm{m}\,\varphi)\sin(\mathrm{m}(\varphi_0-\pi)) \tag{9}$$

Where $R_{mn}^{(1)\prime}(c,\xi)$ and $R_{mn}^{(3)\prime}(c,\xi)$ are the derivative of $R_{mn}^{(1)}(h,\varepsilon)$ and $R_{mn}^{(3)}(h,\xi)$. $R_{mn}^{(3)}(h,\xi)$ is the radial and the angular spheroidal wave functions of the third kind. $R_{mn}^{(3)}(h,\xi)=R_{mn}^{(1)}(h,\xi)+iR_{mn}^{(2)}(h,\xi)$.

In spheroidal coordinate system, vibration velocity can be given by Euler equations，Vibration velocity can be given by Euler equations, and Euler equations can be transformed from rectangular coordinate system to the spheroidal coordinate system is :

$$\vec{u}=-\frac{1}{\rho}\int\nabla p dt=\frac{-2}{j\omega\rho d}\left[g_\xi\frac{\partial p}{\partial\xi}\vec{\xi}+g_\eta\frac{\partial p}{\partial\eta}\vec{\eta}+g_\varphi\frac{\partial p}{\partial\varphi}\vec{\varphi}\right] \tag{10}$$

Where

$$g_\xi=\sqrt{\frac{\xi^2-1}{\xi^2-\eta^2}},g_\eta=\sqrt{\frac{1-\eta^2}{\xi^2-\eta^2}},g_\varphi=\frac{1}{\sqrt{\xi^2-\eta^2}} \tag{11}$$

$$\frac{\partial p}{\partial\xi}=-4\sum_{n=0}^{\infty}\sum_{m=0}^{\infty}i^n\frac{(2-\delta_{0m})R_{mn}^{(1)\prime}(c,\varepsilon_1)}{N_{mn}R_{mn}^{(3)\prime}(c,\varepsilon_1)}S_{mn}(h,\eta_0)R_{mn}^{(3)\prime}(h,\varepsilon)\cdot S_{mn}(h,\eta)\sin(m\varphi)\sin(m(\varphi_0-\pi)) \tag{12}$$

$$\frac{\partial p}{\partial\eta}=-4\sum_{n=0}^{\infty}\sum_{m=0}^{\infty}i^n\frac{(2-\delta_{0m})R_{mn}^{(1)\prime}(c,\varepsilon_1)}{N_{mn}R_{mn}^{(3)\prime}(c,\varepsilon_1)}S_{mn}(h,\eta_0)R_{mn}^{(3)}(h,\varepsilon)\cdot S_{mn}'(h,\eta)\sin(m\varphi)\sin(m(\varphi_0-\pi)) \tag{13}$$

$$\frac{\partial p}{\partial\varphi}=-4\sum_{n=0}^{\infty}\sum_{m=0}^{\infty}i^n\frac{(2-\delta_{0m})R_{mn}^{(1)\prime}(c,\varepsilon_1)}{N_{mn}R_{mn}^{(3)\prime}(c,\varepsilon_1)}S_{mn}(h,\eta_0)R_{mn}^{(3)}(h,\varepsilon)\cdot mS_{mn}(h,\eta)\cos(m\varphi)\sin(m(\varphi_0-\pi)) \tag{14}$$

Thus, the vibration velocity in rectangular coordinate system is:

$$\begin{bmatrix}u_x\\u_y\\u_z\end{bmatrix}=\frac{j}{\omega\rho c}\begin{bmatrix}\xi g_\xi g_\eta & -\eta g_\xi g_\eta & -g_\varphi\\ \xi g_\xi g_\eta & -\eta g_\xi g_\eta & g_\varphi\\ \dfrac{\eta g_\xi^2}{\cos\varphi} & \dfrac{\xi g_\eta^2}{\cos\varphi} & 0\end{bmatrix}\begin{bmatrix}\dfrac{\partial p}{\partial\xi}\cos\varphi\\ \dfrac{\partial p}{\partial\eta}\cos\varphi\\ \dfrac{\partial p}{\partial\varphi}\sin\varphi\end{bmatrix} \tag{15}$$

III Numeral simulation

The numerical calculation parameters we consider(Fig 1)are as follows: The water have sound speed is c_0 =1500m/s and density is ρ =1000kg/ m^3 , the long axis of prolate spheroid is 2.0 m, the short axis is 0.5 m, the distance from the vector sensor to the origin is 1m.

Fig.2 shows relationship between the frequency, direction of incident wave and the amplitude of pressure, vibration velocity of the scattering wave at an observation point (x_0=0, y_0=-1, z_0=0) in rectangular coordinate system. That the pressure and velocity of the vector sensor with prolate spheroid baffle at different frequencies with the condition of the incident wave is in *y-z* plane, the incident plane wave rotates around the prolate spheroid 180° in the *x-y* plane with an interval of 1°($\varphi_0 = 3\pi/2$, $\theta_0 \in (0,\pi)$), and the frequencies is from 1 kHz to 5 kHz.

As shown in Fig. 2, the vibration velocity in the y axis and pressure are the same, only the different amplitude. From the Eq(15) ,the vibration velocity in the z axis is 0. As frequency increased, the circular become more and more aberration. Since the soft water surface, the prolate spheroid has little effect on the horizontal incident wave. In the vertical, the pressure and vibration velocity in y axis scattering acoustic field will be maximum. The vibration velocity in *x* axis scattering acoustic field will be minimum.

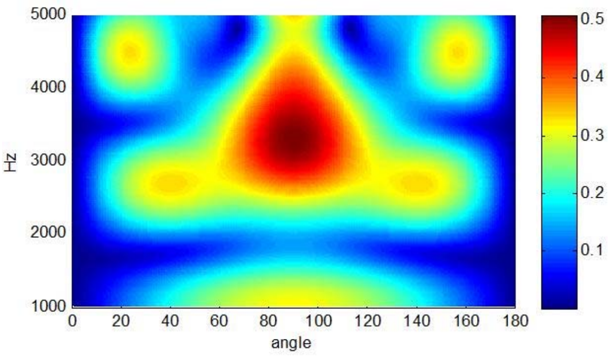

(a) pressure

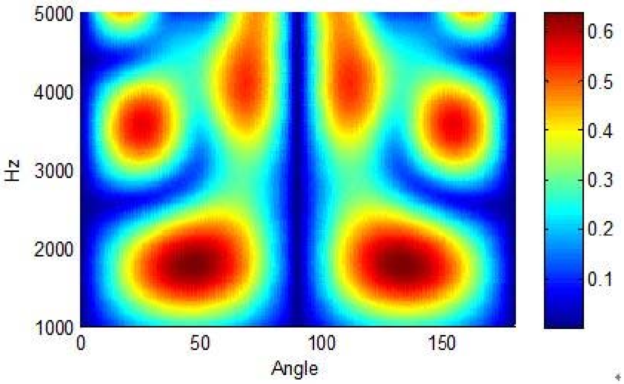

(b) vibration velocity in the *x* axis

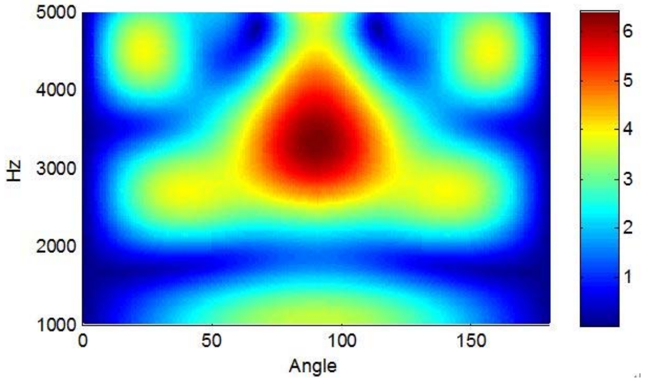

(c) vibration velocity in the y axis

Fig.3 The directivity of Prolate Spheroid acoustic Scattering with incident wave in the y-z plane, $\theta_0 = \pi/2$ $\varphi_0 \in (\pi, 2\pi)$. Spheroid's major axis a=2, the minor axis b=0.5, the vector sensor at the bottom of the Prolate Spheroid(x_0=0, y_0=-1, z_0=0).

Fig. 3 shows the directivity of acoustic scattering pressure and vibration velocity of the scattering wave at an observation point (x_0=0, y_0=-1, z_0=0) in rectangular coordinate system. That the directivity of pressure and velocity of the vector sensor with prolate spheroid baffle at different frequencies with the condition of the incident wave is in *x-y* plane, and the incident plane wave rotates around the prolate spheroid 180° in the *x-y* plane with an interval of 1°. $\theta_0 = \pi/2$, $\varphi_0 \in (\pi, 2\pi)$. The directivity of acoustic scattering pressure and vibration velocity in the *x* axis and y axis is shown in Fig.3(a)(b)(c). The vibration velocity in the z axis is 0. At 1.2 kHz the directivity of pressure is approximate to circular. As frequency increased, the circular become more and more aberration. The directivity of acoustic scattering pressure and vibration velocity in y axis of the scattering wave is the same.

Fig. 4 shows the directivity of acoustic scattering pressure and vibration velocity of the scattering wave at an observation point (x_0=0, y_0=-1, z_0=0)in rectangular coordinate system. That the directivity of pressure and velocity of the vector sensor with prolate spheroid baffle at different frequencies with the condition of the incident wave is in *y-z* plane, and the incident plane wave rotates around the prolate spheroid 180° in the *x-y* plane with an interval of 1°. $\varphi_0 = 3\pi/2$, $\theta_0 \in (0,\pi)$. The vibration velocity in the *x* axis is 0. The directivity of acoustic scattering pressure and vibration velocity in the *y* axis and *z* axis is shown in Fig. 4 (a)(b)(c). The directivity of acoustic scattering pressure and vibration velocity in y axis of the scattering wave is the same.

Compare with Fig.3, the directivity of acoustic scattering pressure are more sharp when the incident plane wave in *x-y* plane. Because of the soft water surface when the incident wave parallel to the horizontal plane, the acoustic scattering pressure will be reduced to a minimum.

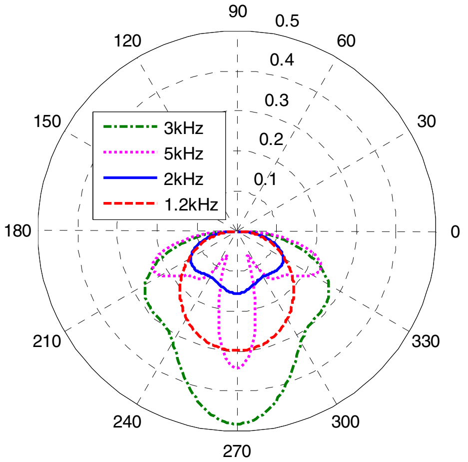

(a) pressure

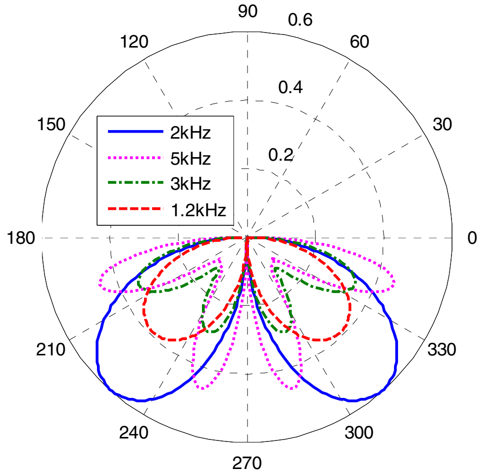

(b) vibration velocity in the *x* axis

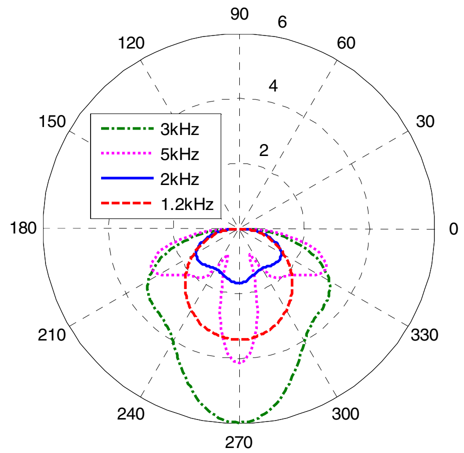

(c) vibration velocity in the y axis

Fig.3 The directivity of Prolate Spheroid acoustic Scattering with incident wave in the y-z plane, $\theta_0 = \pi/2$ $\varphi_0 \in (\pi, 2\pi)$. Spheroid's major axis a=2, the minor axis b=0.5, the vector sensor at the bottom of the Prolate Spheroid(x_0=0, y_0=-1, z_0=0).

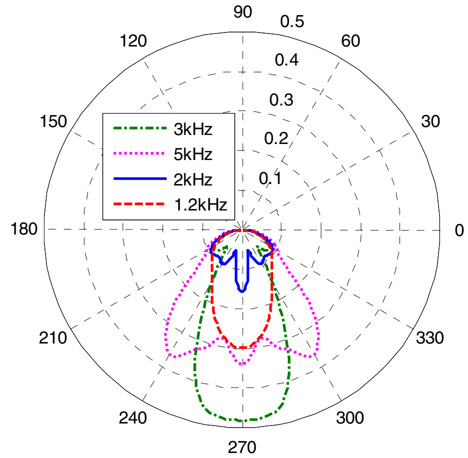

(a) pressure

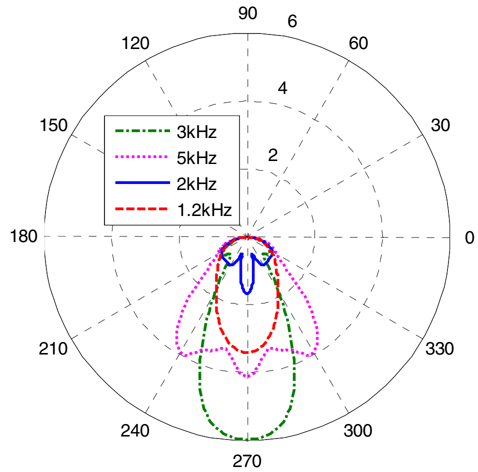

(b) vibration velocity in the y axis

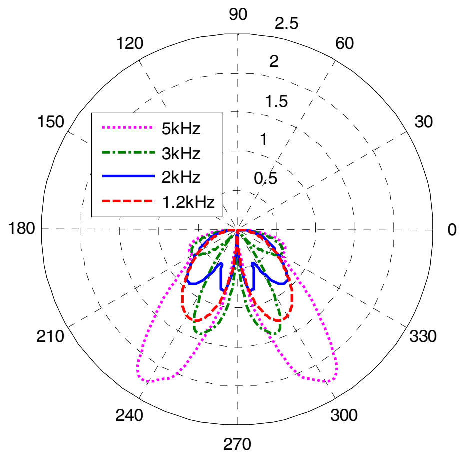

(c) vibration velocity in the z axis

Fig.4 The directivity of Prolate Spheroid acoustic Scattering with incident wave in the y-z plane, $\varphi_0 = 3\pi/2$, $\theta_0 \in (0, \pi)$. Spheroid's major axis a=2, the minor axis b=0.5, the vector sensor at the bottom of the Prolate Spheroid(x_0=0, y_0=-1, z_0=0).

IV Conclusion

The Prolate Spheroid Model at the water surface has been developed for vessel scattering acoustic field calculation. The Scattering Acoustic pressure and vibration velocity field's calculated results have been presented.

From the calculation of result, the vibration velocity in the z axis is 0 when the incident plane wave in *x-y* plane, the vibration velocity in the *x* axis is 0 when the incident plane wave in *y-z* plane. In the condition of soft water surface, the prolate spheroid has little effect on the horizontal incident wave. In the vertical, the cattering acoustic field will be maximum. So one possible application is in sub-bottom profiling, the vessel and water surface scattering acoustic waves maybe influence the accuracy of sub-bottom's acoustically parameter estimation.

ACKNOWLEDGMENT

Research are funded by National Natural Science Foundation of China (No.41327004, No.41306182 and 61401112).

REFERENCES

[1] G. C. Gaunaurd and M. F. Werby, ''Interpretation of the three-dimensional sound fields scattered by submerged elastic shells and rigid spheroidal bodies,'' J. Acoust. Soc. Am. **84**, 673–680 ~1988.

[2] 1P. C. Waterman, ''New formulation of acoustic scattering,'' J. Acoust. Soc. Am. **45**, 1417–1429 ~1969!.

[3] V. K. Varadan, V. V. Varadan, L. R. Dragonette, ''Computation of rigid body scattering by prolate spheroids using the T-matrix approach,'' J. Acoust. Soc. Am. **71**, 22–25 ~1982.

[4] L. Flax and L. R. Dragonette, ''Analysis and computation of the acoustic scattering by an elastic prolate spheroid obtained from the T-matrix formulation,'' J. Acoust. Soc. Am. 71, 1077–1082 ~1982.

[5] Z. Ye, E. Hoskinson, R. K. Dewey, L. Ding,''A method for acoustic scattering by slender bodies. I. Theory and verification,'' J. Acoust. Soc. Am. 102, 1964–1976 ~1997.

[6] Zhuo Lin-kai, Analyzing Acoustic Scattering of Elastic Objects Using Coupled FEM-BEM Technique. Journal of Shanghai Jiao Tong University. Vol.43 No.8 Aug. 2008

[7] Barton J P, Nicholas L W, Zhang H F, et al. Near-field calculations for a rigid spheroid with an arbitrary incident acoustic field. J Acoust Soc Am, 2003, 113(3): 1216−1222

[8] JianFei Ji, GuoLong Liang, Kai Liu. "Influences of soft prolate spheroidal baffle on Directivity of Acoustic Vector Sensor", 2010 IEEE International Conference on Information and Automation (ICIA), ,ICIA 2010, 650-654.

[9] JianFei Ji, GuoLong Liang, Yan Wang and WangSheng Lin. Influences of prolate spheroidal baffle of sound diffraction on spatial directivity of acoustic vector sensor, SCIENCE CHINA Technological Sciences, Volume 53, Number 10, OCT., 2010, 2846-2852.

[10] Sheng Xueli ,Guo Longxiang ,Liang Guolong. Study on the directivity of the vector sensor with spherical soft baffle plate[J].Technical Acoustics , 2002(9) :56 - 60.

[11] J. Fawcett, ''Complex-image approximations to the half-space acoustoelastic Green's function,'' J. Acoust. Soc. Am. 108, 2791–2795 ~2000.

[12] J. Fawcett, ''A method of images for a penetrable acoustic waveguide,'' J.Acoust. Soc. Am. **113**, 194–204 ~2003.

[13] J. Fawcett, L Raymond "Evaluation of the integrals of target/seabed scattering using the method of complex images'' Journal of the Acoustical Society of America, 2003, 114(3): 1406-1415.

[14] 6Y. L. Li and M. J. White, ''Near-field computation for sound propagation above ground—Using complex image theory,'' J. Acoust. Soc. Am. 99, 755–760 ~1996.

[15] G. C. Gaunaurd and H. Huang, ''Acoustic scattering by a spherical body near a plane boundary,'' J. Acoust. Soc. Am. **96**, 2526–2536 ~1994!.

[16] H. Huang and G. C. Gaunaurd, ''Scattering of a plane acoustic wave by a spherical elastic shell near a free surface,'' Int. J. Solids Struct. **34**, 591–602 ~1997.

[17] Flammer.C., Spheroidal Wave Functions. Standford University Press, Standford,CA(1957).